nature nanotechnology

ARTICLES

https://doi.org/10.1038/s41565-019-0578-8

Positive and negative chemotaxis of enzyme-coated liposome motors

Ambika Somasundar[1], Subhadip Ghosh[2], Farzad Mohajerani[1], Lynnicia N. Massenburg[3], Tinglu Yang[2], Paul S. Cremer[2]*, Darrell Velegol[1]* and Ayusman Sen[2]*

The ability of cells or cell components to move in response to chemical signals is critical for the survival of living systems. This motion arises from harnessing free energy from enzymatic catalysis. Artificial model protocells derived from phospholipids and other amphiphiles have been made and their enzymatic-driven motion has been observed. However, control of directionality based on chemical cues (chemotaxis) has been difficult to achieve. Here we show both positive or negative chemotaxis of liposomal protocells. The protocells move autonomously by interacting with concentration gradients of either substrates or products in enzyme catalysis, or Hofmeister salts. We hypothesize that the propulsion mechanism is based on the interplay between enzyme-catalysis-induced positive chemotaxis and solute–phospholipid-based negative chemotaxis. Controlling the extent and direction of chemotaxis holds considerable potential for designing cell mimics and delivery vehicles that can reconfigure their motion in response to environmental conditions.

Directional migration in response to specific signals is critically important in biological systems. Chemotaxis (the movement towards or away from chemical stimuli) enables living cells to move towards food or escape away from toxins, exchange chemical signals with the environment, transport cargo and coordinate collective behaviour such as biofilm formation and tissue development[1,2]. Inspired by biology, scientists have created a variety of synthetic materials that exhibit self-propulsion based on chemical and biochemical reactions[3–5]. The movement arises from harnessing chemical free energy derived from catalysis. A fundamental question that arises is whether the direction of movement of such materials can be controlled through the interplay between an imposed external chemical gradient and/or a self-generated gradient due to catalytic turnover. Enabling directional control over the motion has important implications in the fields of biological transport and the design of 'smart' autonomously moving motors, that can find applications in nanorobotics[6], nanoscale assembly[2], chemical/biochemical sensing[7–9] and as drug or cargo delivery vehicles[10].

We have previously shown that enzymes, such as catalase, urease and hexokinase, as well as the corresponding enzyme-coated hard particles, move directionally towards regions of higher substrate concentrations, exhibiting positive chemotaxis[11–14]. Positive chemotaxis arises from a thermodynamic driving force that lowers the chemical potential of the system due to favourable substrate binding. Substrate gradient-induced enzyme chemotaxis by cross-diffusion transfers enzymes towards regions of higher substrate concentration[14,15]. While this positive chemotactic movement has been fairly well studied, the ability to move away from specific chemicals, negative chemotaxis, is less well-established[16,17], and systems that show both positive and negative chemotaxis have not been described. In this paper, we report that active liposomes exhibit both positive and negative chemotactic movement depending on specific chemical cues. We show (1) positive chemotactic movement of catalase-coated liposomes, (2) negative chemotactic movement of urease-coated liposomes and (3) both positive and negative chemotaxis of ATPase-bound liposomes. Furthermore, through a combination of experiments, we demonstrate that the movement of the liposomes is governed by their interactions with the surrounding solute gradients. Having ruled out electrolyte diffusiophoresis, osmophoresis, thermophoresis and density effects for negative chemotaxis, we show that negative chemotaxis arises from repulsive interactions between specific ions and the phospholipid groups of the liposome, a hitherto unrecognized extension of the Hofmeister effect[18–21]. Indeed, the direction and extent of chemotaxis of liposomes can be controlled by systematically changing the chemical composition of the imposed gradient. Phospholipids and other amphiphiles are ubiquitous constituents of cell membranes and synthetic vesicles[22], and their directed motion in response to specific ionic gradients has important implications for cell motility, both biological and synthetic. Vesicle could be used to design biocompatible drug or cargo autonomous delivery vehicles[23–26]. As an example, positive chemotaxis has been employed to transport polymerosomes across the blood–brain barrier[23]. Equally important, our work herein on the Hofmeister effect suggests its possible role in directional transport of biomolecules and natural vesicles in physiological environments.

Design of the experimental system

In our experiments, we examined the directed movement of enzyme-coated liposomes in microfluidic channels (see Methods section for details). Figure 1a is a schematic diagram of an enzyme-coated liposome placed in a gradient of the substrate. A three-inlet one-outlet polydimethylsiloxane (PDMS) device with dimensions of 4 cm (length) × 360 μm (width) × 100 μm (height) was used to visualize liposome chemotaxis under confocal microscopy (Fig. 1b)[9,27]. Enzyme-coated liposomes were flown through the middle channel, and the substrate and buffer were flown in each of the side channels, respectively. With known flow rates and channel dimensions, the diffusion time and interaction time between the liposomes and substrates can be controlled. Optical scans were taken across the main channel width, 38 mm downstream from the three-channel inlet

[1]Department of Chemical Engineering, The Pennsylvania State University, University Park, PA, USA. [2]Department of Chemistry, The Pennsylvania State University, University Park, PA, USA. [3]Department of Biochemistry and Molecular Biology, The Pennsylvania State University, University Park, PA, USA. *e-mail: psc11@psu.edu; velegol@psu.edu; asen@psu.edu

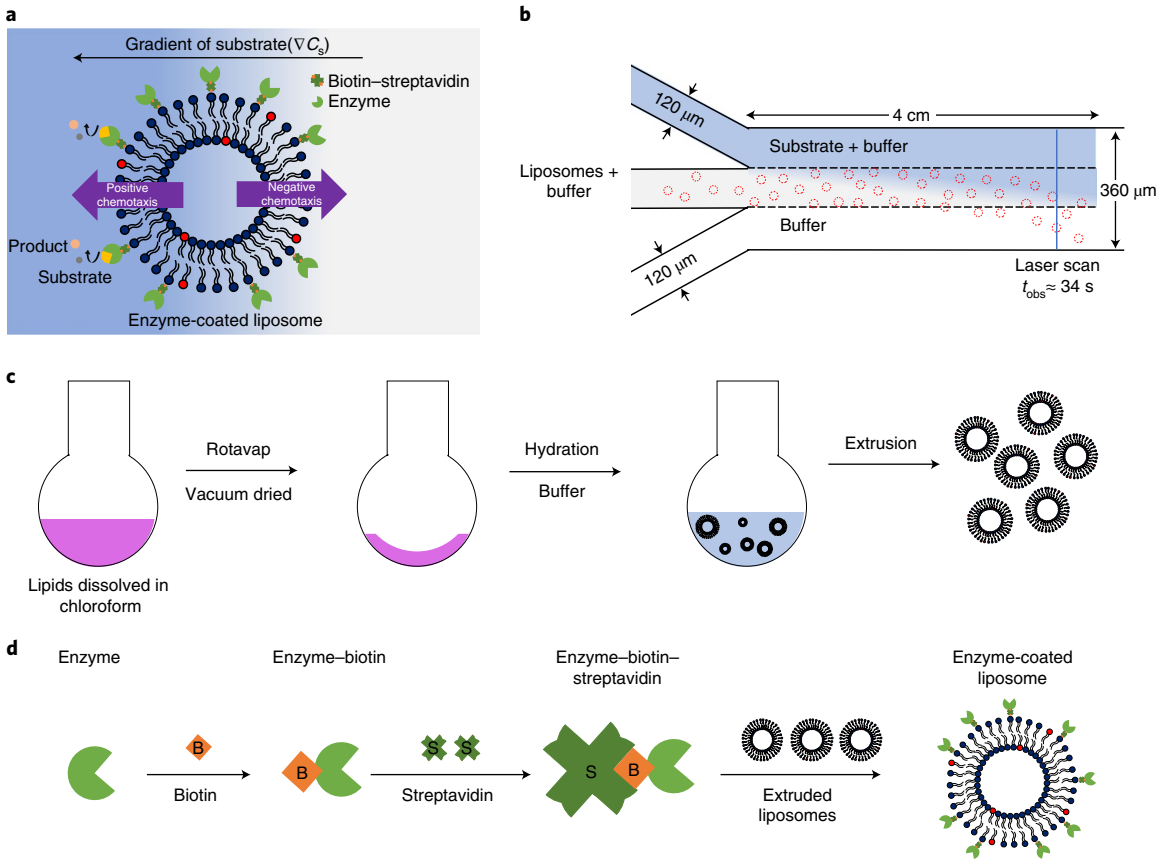

Fig. 1 | Schematic illustration of liposomes in the gradients and the experimental set-up. **a**, Migration of enzyme-coated liposomes towards or away from the substrate based on enzymatic propulsion or solute interactions. The lipid constituents include: Egg Liss Rhod PE (the red-headed lipid) as fluorescent marker, DSPE-PEG (2000) biotin (the blue-headed lipid with attached enzyme) and L-α-phosphatidylcholine lipids (the blue-headed lipid) for the remainder of the liposomes. **b**, The three-inlet one-outlet microfluidic device. Typical flow rate of 50 μl h^{-1} through each inlet was used to maintain the interaction time, t_{obs} ≈ 34 s. **c**, Experimental procedure used to make 100 nm liposomes through thin-film hydration and extrusion. **d**, Experimental procedure of attaching enzymes to the external surface of the liposomes through biotin–streptavidin conjugation.

using a confocal laser scanning microscope. The interaction time of ~34 s was maintained by setting the flow rate of the syringe pump to 50 μl h^{-1} for each inlet for all the microfluidic device experiments. Chemotactic shifts of liposomes were measured perpendicular to the direction of flow (see Supplementary Information for details). The fluorescent intensity profiles from each experiment were normalized to values between 0 and 1 with the minimum intensity being 0 and the maximum intensity being 1. As the fluorescently tagged liposomes are in the middle of the channel, we obtain the maximum intensity in the centre channel and we get a gradient of decreasing fluorescence intensity going from the middle to either of the side channels, in part due to Fickian diffusion of liposomes over the ~34 s it takes them to flow 38 mm downstream.

Catalase-coated liposomes undergo positive chemotaxis

Catalase is an enzyme with a high turnover number (~10^5 s^{-1}) that converts hydrogen peroxide into water and oxygen[28]. Consistent with the reported chemotaxis of catalase molecules[11] and catalase-coated particles[12], positive chemotactic propulsion of catalase-coated liposomes was seen (Fig. 2a). In this figure, the dashed vertical lines represent the interfaces between the three input channels and they break the main channel into three regions: left, middle and right. When comparing Fig. 1b with Fig. 2a,b, the top of the microfluidic channel corresponds to the left region and the bottom corresponds to the right region. When we flowed 2 mM hydrogen peroxide in the top channel, catalase-coated liposomes in the middle channel and the buffer in the bottom channel, we observed a positive chemotactic shift of ~5 μm for the liposomes towards the H_2O_2. Due to the formation of oxygen bubbles, we were unable to obtain the shift of the liposomes as a function of H_2O_2 concentration. After confirming that catalase shows a positive chemotactic shift when bound to the liposome, we wanted to determine if other enzyme molecules that show positive chemotaxis will also demonstrate positive shifts when attached to liposomes.

Urease-coated liposomes undergo negative chemotaxis

Urease is another enzyme that shows positive chemotaxis in a gradient of its substrate, as does urease-coated solid particles[11,12]. It was, therefore, surprising to see that liposomes coated with urease shift away from high concentrations of urea (Fig. 2b). As we increased the substrate concentration, we observed an increase in negative chemotactic shift (Fig. 2c). To confirm that the negative chemotactic movement is due to the reaction of urease with its substrate (equation (1)), inactive liposomes (that is, liposomes with no attached enzymes) were flowed with the reactant (urea) and products ($2NH_4^+ + CO_3^{2-}$). The substrate urea does not cause any additional movement other than Fickian diffusion over the concentration range of 0–150 mM urea (blue data points in Fig. 2c). Notably, the product, $(NH_4)_2CO_3$, also causes a negative chemotactic shift for both inactive and urease-coated liposomes as shown in Fig. 2d.

$$(NH_2)_2CO + 2H_2O \rightarrow 2NH_4^+ + CO_3^{2-} \quad (1)$$

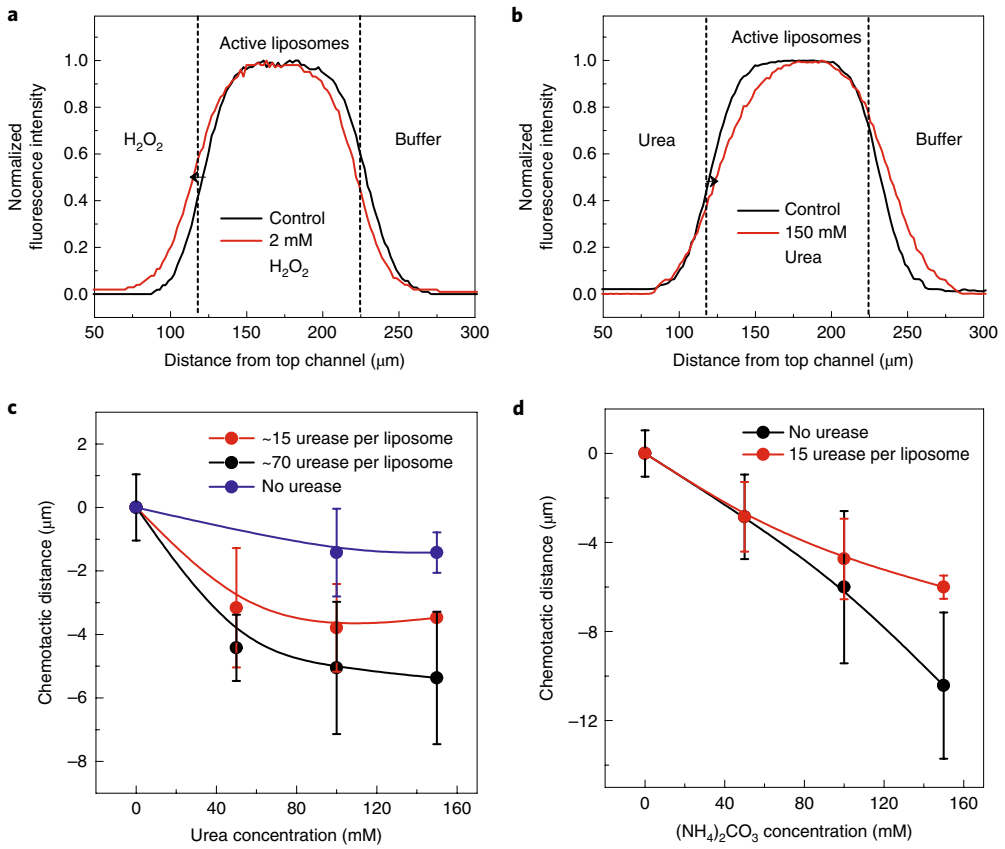

Fig. 2 | Catalysis-induced positive chemotaxis of catalase-coated liposomes and negative chemotaxis of urease-coated liposomes. a,**b**, Fluorescence intensity profiles of catalase-coated liposomes and urease-coated liposomes in imposed gradients of their respective substrates. The arrow in **a** indicates that active catalase-coated liposomes move towards the substrate (positive chemotaxis), with [H_2O_2] = 2 mM, [PBS] = 10 mM. The arrow in **b** indicates that the active urease-coated liposomes move away from the substrate (negative chemotaxis), with [urea] = 150 mM, [phosphate buffer] = 100 mM (pH 7.2). **c**, Chemotactic migration of inactive liposomes, with no attached enzymes (blue), active liposomes with high enzyme coverage (~70 enzymes per liposome, see Supplementary Fig. 4) (black), and active liposomes with lower enzyme coverage (estimated ~15 enzymes per liposome) (red) in response to different concentrations of the substrate, urea. [Phosphate buffer] = 100 mM (pH 7.2). **d**, Negative chemotactic migration of inactive liposomes (black) and active liposomes with low urease coverage (red) in response to different concentrations of product, $(NH_4)_2CO_3$. [Phosphate buffer] = 100 mM (pH 7.2). Error bars represent 90% confidence intervals based on three independent runs.

It is clear from the above observations that it is the product of urea hydrolysis by urease that is responsible for the observed negative chemotaxis of both inactive and urease-coated liposomes. The higher the starting concentration of urea, the faster the product formation is, which leads to more negative chemotaxis (Fig. 2c).

ATPase-bound liposomes undergo tunable chemotaxis

ATPase is a transmembrane enzyme that is directly inserted into the phospholipid bilayer (see Methods section for preparation details). ATPase is known to dephosphorylate adenosine triphosphate (ATP) to adenosine diphosphate (ADP) plus a phosphate ion (Pi). When the ATPase-bound liposomes were flowed through the microfluidic channel in the presence of an ATP gradient, they exhibited a positive chemotactic shift up the gradient at all concentrations that were tested (0.1 to 10 mM). The shift went through a maximum of 11.4 μm at 0.5 mM ATP (Fig. 3a, red data points). As the concentration of ATP supplied is further increased, the magnitude of positive chemotaxis decreases due to a combination of product inhibition and negative chemotaxis due to the self-generated gradients of ADP and Pi[29,30]. In addition, when we ran control experiments with inactive liposomes (without any ATPase bound to the membrane), in the presence of an ATP concentration gradient the liposomes showed a negative chemotactic shift (Fig. 3a, black data points). This opposite trend for inactive liposomes (as compared to the active liposomes) was found to increase with increasing ATP concentration. We also carried out control experiments by flowing ATPase-bound liposomes in the presence of the products, ADP and Pi. The liposomes showed similar negative chemotaxis behaviour in a gradient of the products as well (Fig. 3b). In the case of active liposomes, however, enzymatic propulsion dominates over the repulsive interaction, propelling the liposomes up the ATP gradient. Nevertheless, the two forces compete and, therefore, the chemotactic shift goes through a maximum as the ATP concentration is increased. Finally, in the presence of ADP and Pi only, ATPase-bound liposomes show negative chemotaxis. Thus, the directional motility of the ATPase-bound liposomes can be controlled by the choice of imposed chemical gradients.

The results from the three different enzyme-coated liposomes indicate that we are able to control the direction of motion of active liposomes either towards or away from high concentrations of substrate, as opposed to previously shown cases of only positive chemotactic movement for enzymes and enzyme-coated hard particles. This suggests that there is an additional mechanism of movement that acts on these soft liposomal particles. We systematically rule out electrolyte diffusiophoresis, osmophoresis, thermophoresis and density effects for negative chemotaxis, and propose a mechanism to move particles directionally based on solute–phospholipid interactions.

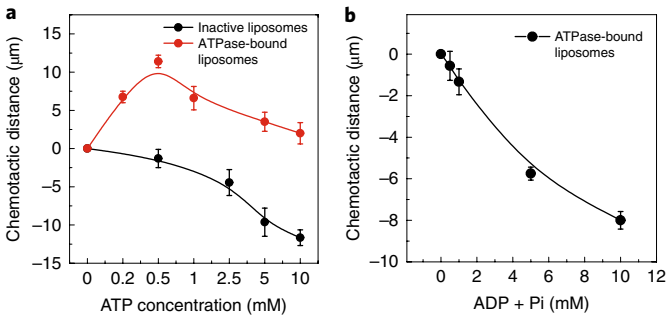

Fig. 3 | Reconfiguration of direction of movement in ATPase-bound liposomes. a, Chemotactic migration of inactive (black line) and active (red line) liposomes in response to different concentration gradients of the substrate, ATP. [Mg^{2+}] = 1 mM, [HEPES buffer] = 10 mM (pH = 7.8). **b**, Negative chemotactic migration of active liposomes in response to different concentration gradients of the products, ADP + Pi. [Mg^{2+}] = 1 mM, [HEPES buffer] = 10 mM (pH = 7.8). Mg^{2+} was added as a cofactor in all three channels to ensure maximum activity of the enzyme. Error bars represent 90% confidence intervals based on three independent runs.

Ruling out alternative transport mechanisms

Recently, the movement of liposomes through an electrolyte diffusiophoretic mechanism was demonstrated both experimentally and theoretically[31–33]. The concentration gradient of electrolytes imposed on a charged liposome gives rise to the movement of the particles via electrophoresis through spontaneously generated electric fields and chemiphoresis by generating pressure fields within the Debye length of the particles[34]. Based on the zeta potential of the liposomes (ζ), the diffusivity difference factor (β) and the concentration gradient of the salt (∇C), the liposomes move either towards or away from a region of high concentration of electrolyte.

When we tested the zeta potential of liposomes in buffer, they were found to have a zeta potential of only −2 mV. The zeta potential becomes slightly more negative (−4 mV) with the addition of 100 mM NH_4HCO_3. To ensure that these low zeta potential values indeed do not cause electrolyte diffusiophoretic flows, we performed microfluidic experiments using two salts: one with a positive β value (NH_4HCO_3) and one with a negative β value (NaCl). Here β is the diffusivity difference factor that depends on the nature of the anion versus the cation and is expressed in terms of the diffusion coefficients of the constituent ions. For a Z_+:Z_- salt, it is given by[35]

$$\beta = \frac{D_+ - D_-}{D_+ + D_-} \quad (2)$$

where D_+ is the diffusion coefficient of the cation and D_- is the diffusion coefficient of the anion.

For NH_4HCO_3, the β value is +0.245, while for NaCl it is −0.207. If the mechanism of liposome migration is electrolyte diffusiophoretic, the liposomes should show movement in the opposite direction when placed in a gradient of NaCl as compared to a gradient of NH_4HCO_3. We tested the motion of the liposomes in the presence of both salts and found a negative chemotactic shift for NH_4HCO_3 but no shift for NaCl (Fig. 4). This suggests that electrolyte diffusiophoresis is not a driving force for the observed motion in our system, presumably because the presence of the buffer reduces the double layer around the liposomes.

Solutal buoyancy differences between reactants and products of an enzyme can cause self-powered fluid flows in enzyme micropumps[36,37]. To rule out density-driven flow of liposomes in our system, we performed microfluidic experiments by replacing the liposomes with 200 nm FluoSpheres amine-functionalized polystyrene particles. The fluorescent particles were flowed in the middle channel, while the substrate (urea, NH_4HCO_3) and buffer were flowed through the left-hand and right-hand side channels, respectively. In the control case, both side channels contain only buffer. The fluorescence intensity profiles are rougher than the case of 100 nm liposomes. Since, the fluorescent particles are larger, they appear as high-intensity spikes in the channel rather than smooth curves as is the case for the liposomes. Nevertheless, it is clear that there were no negative shifts (movement away) from the interface between the substrate and particles (left dashed vertical lines on the image) as shown in Fig. 5a,b. This rules out density-driven migration in our system.

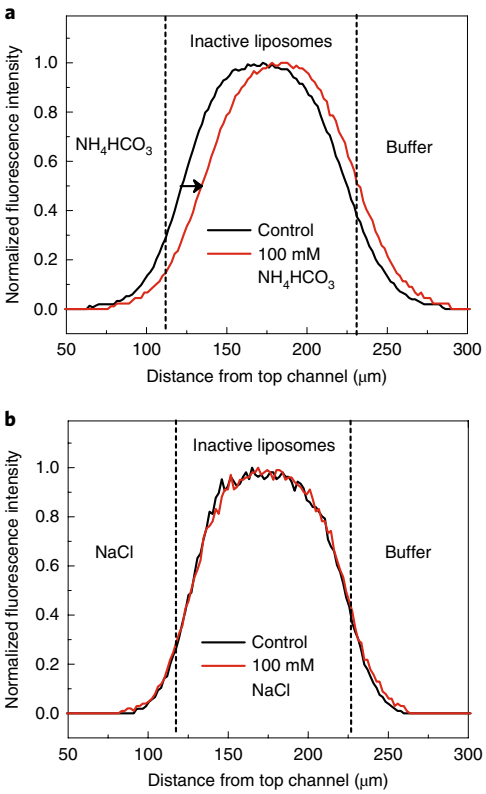

Fig. 4 | Ruling out electrolyte diffusiophoretic transport. a,**b**, Fluorescence intensity profile of inactive liposomes in an imposed gradient of NH_4HCO_3 (**a**) and NaCl (**b**), both in 10 mM PBS buffer. The arrows indicate that the inactive liposomes move away from the imposed gradient of NH_4HCO_3 but not NaCl. The initial concentrations of NH_4HCO_3 and NaCl introduced into the left channel were each 100 mM.

The movement of semipermeable vesicles towards regions of lower solute concentration, when placed in a gradient of an impermeable solute, is termed osmophoresis[38]. Due to the difference in osmotic pressure (solute concentration) inside and outside the semipermeable colloid, the liposome expels water from the side facing the higher concentration and admits water from the opposite side. This propels the liposome towards a region of lower solute concentration or osmotic pressure. The osmophoretic velocity is directly dependent on the size of the colloid, water permeability and the solute gradient across the liposome[34]. This mechanism has been experimentally explored and tested[38,39]. Despite the qualitative agreement, it has been shown that the predicted velocity by this mechanism was smaller than the observed vesicle motion, by at least three orders of magnitude[39].

We tested the osmophoresis hypothesis by comparing the experimental chemotactic shifts with theoretical osmophoretic velocities for a simple case, that is, migration of inactive liposomes (liposomes without enzymes) in a gradient of a polar uncharged solute,

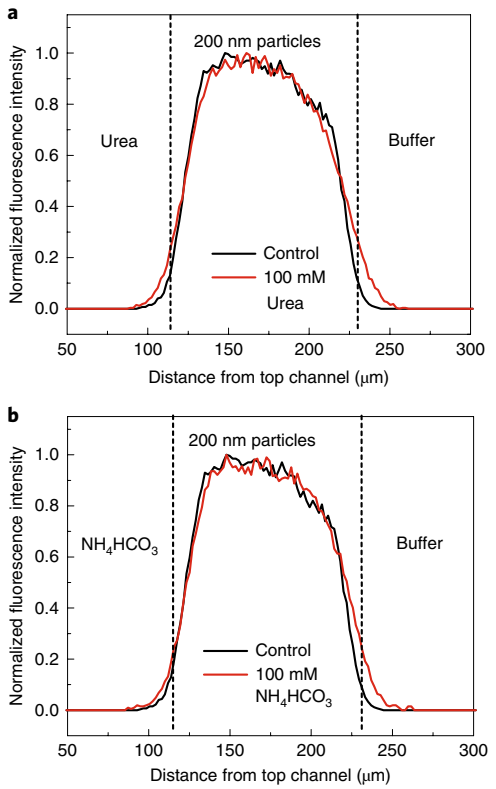

Fig. 5 | Ruling out density-driven transport. a,**b**, Fluorescent intensity profiles of solid 200 nm particles in the presence of an imposed gradient of urea (**a**) and ammonium bicarbonate (**b**), both in 100 mM PBS buffer. There is no movement of the particles in the imposed gradients suggesting that the mechanism of negative chemotaxis is not density driven.

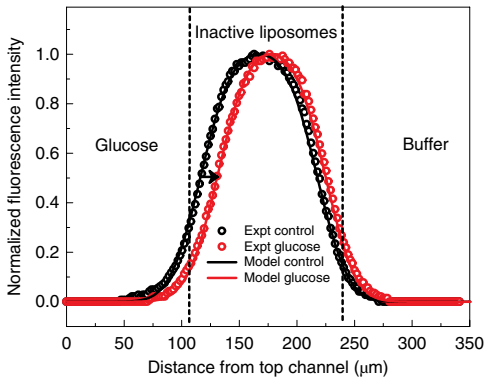

Fig. 6 | Chemotactic movement of inactive liposomes in glucose. Normalized fluorescence intensity for the negative chemotactic shift of liposomes in a concentration gradient of glucose (150 mM in the left channel) in 10 mM PBS buffer, obtained through experiments (circles) and modelling (lines).

glucose (see Supplementary Fig. 5). The system was modelled using COMSOL Multiphysics (v.5.3) (see Supplementary Information for details). Under steady-state conditions, the concentration profile of the liposome in the presence of an impermeable solute gradient (C_S) was modelled by incorporating the theoretical osmophoretic velocity (U_{osm}) into the flux ($\mathbf{J}_L$) equation as follows:

$$\nabla \cdot \mathbf{J}_L = 0 = -D_L \nabla^2 C_L + \mathbf{u} \nabla C_L + \nabla \cdot (U_{osm} C_L) \quad (3)$$

where C_L and D_L are the concentration and diffusion coefficients of the liposomes, $\mathbf{u}$ is the fluid velocity in the microfluidic channel and ∇ is the gradient operator. The osmophoretic velocity is given by[34]

$$U_{osm} = -\frac{aL_p RT \nabla C_s}{2} \quad (4)$$

where a is the radius of the particle, L_p is the hydraulic permeability of the membrane, R is the universal gas constant, T is the temperature, ∇C_s is the solute concentration gradient and $RT\nabla C_s$ is the gradient of osmotic pressure. Using this approach, close agreement between experiments and simulation is only possible by introducing a large correction factor of 8×10^4 into the equation for the theoretical osmophoretic velocity (Fig. 6). This substantial discrepancy between theory and experiment is similar to that reported[39], and indicates that the osmophoretic hypothesis cannot explain the observed negative chemotactic movement. It should also be noted that the sizes of the liposomes do not change significantly in the presence of either the reactant (urea) or the product ($(NH_4)_2CO_3$) (Supplementary Fig. 2).

Since the enzymes employed in this study catalyse exothermic reactions, a substrate gradient can result in a gradient in temperature, leading to thermophoresis. However, this is unlikely for the following reasons. As shown previously, positive chemotaxis, which occurs even with enzymes catalysing endothermic reactions, is the result of a thermodynamic driving force that lowers the chemical potential of the system due to favourable substrate binding[14,15]. Negative chemotaxis was observed even in the absence of a reaction, for example in the presence of the reaction products (Figs. 2d, 3b) and for inactive liposomes (Fig. 4a).

Transport due to Hofmeister-type ionic interactions

We have examined the interactions of the lipid bilayer with salts and osmolytes. Solutes can interact with surfaces through excluded volume effects, dipole interactions, ion pairing interactions or van der Waals forces[18,21]. The Hofmeister (or lyotropic) series is a classification of anions and cations according to their ability to 'salt-out' (aggregate or precipitate) or 'salt-in' (solubilize) organic and biomolecules[21,40,41–47]. The effect is due to the size, shape, hydration thermodynamics, charge distribution, hydrogen bonding capability and hydrophobicity of these ions[18–21]. Ions and neutral osmolytes (for example, carbonate and sulfate ions, and glucose) that are well-hydrated do not associate well with hydrophobic organic and biomolecules, and repel them.

The extent and direction of chemotactic movement depends on very specific interactions between the phospholipids and the solute. As described in the Supplementary Information (Supplementary Fig. 6), we also observe negative chemotaxis with liposomes made of 1-palmitoyl-2-oleoyl-glycero-3-phosphocholine (POPC): 1-palmitoyl-2-oleoyl-sn-glycero-3-phosphoethanolamine (POPE) in the molar ratio 70:30 in an $(NH_4)_2CO_3$ gradient. Particles that lack the specific phospholipid coat do not exhibit the same movement control (Fig. 5). However, solid silica particles, when decorated with surface phospholipid bilayers, also show similar movement to liposomes (Supplementary Fig. 7). This interaction depends on the chemical composition of the liposomes and the solutes present, and constitutes a novel propulsion mechanism. As noted, even neutral well-hydrated solutes (for example, glucose, see Fig. 6 and Supplementary Fig. 5) also induce negative chemotaxis of the vesicles.

Conclusions

We have demonstrated the ability to predict the direction of autonomous motion of enzyme-coated liposomes. The observed directionality is based on the interplay between enzymatic-catalysis-induced

positive chemotaxis and solute–phospholipid-interaction-based negative chemotaxis. Regulating the extent and direction of chemotaxis holds considerable potential for the design of nanomotors that can reconfigure their motion in response to environmental conditions. As an example, we have shown that the directed motion of ATPase-bound liposomes can be altered in response to the concentration of the substrate ATP supplied to the liposomes (Fig. 3). Soft nanocapsules with controlled directional movement in self-generated and/or biologically relevant external solute gradients allow the fabrication of novel cell mimics and cargo delivery vehicles.

Online content

Any methods, additional references, Nature Research reporting summaries, source data, extended data, supplementary information, acknowledgements, peer review information; details of author contributions and competing interests; and statements of data and code availability are available at https://doi.org/10.1038/s41565-019-0578-8.

Received: 25 September 2018; Accepted: 15 October 2019;
Published online: 18 November 2019

References

1. Xu, C., Hu, S. & Chen, X. Artificial cells: from basic science to applications. *Biochem. Pharmacol.* **19**, 516–532 (2016).
2. Wang, W., Duan, W., Ahmed, S., Sen, A. & Mallouk, T. E. From one to many: dynamic assembly and collective behavior of self-propelled colloidal motors. *Acc. Chem. Res.* **48**, 1938–1946 (2015).
3. Tu, Y. et al. Mimicking the cell: bio-inspired functions of supramolecular assemblies. *Chem. Rev.* **116**, 2023–2078 (2016).
4. Küchler, A., Yoshimoto, M., Luginbühl, S., Mavelli, F. & Walde, P. Enzymatic reactions in confined environments. *Nat. Nanotechnol.* **11**, 409–420 (2016).
5. Kumar, B. V. V. S. P., Patil, A. J. & Mann, S. Enzyme-powered motility in buoyant organoclay/DNA protocells. *Nat. Chem.* **10** (2018), 1154–1163.
6. Sengupta, S., Ibele, M. E. & Sen, A. Fantastic voyage: designing self-powered nanorobots. *Angew. Chem. Int. Ed.* **51**, 8434–8445 (2012).
7. Duan, W. et al. Synthetic nano- and micromachines in analytical chemistry: sensing, migration, capture, delivery, and separation. *Annu. Rev. Anal. Chem.* **8**, 311–333 (2015).
8. Hong, Y., Blackman, N. M. K., Kopp, N. D., Sen, A. & Velegol, D. Chemotaxis of nonbiological colloidal rods. *Phys. Rev. Lett.* **99**, 1–4 (2007).
9. Baraban, L., Harazim, S. M., Sanchez, S. & Schmidt, O. G. Chemotactic behavior of catalytic motors in microfluidic channels. *Angew. Chem. Int. Ed.* **52**, 5552–5556 (2013).
10. Patra, D. et al. Intelligent, self-powered, drug delivery systems. *Nanoscale* **5**, 1273–1283 (2013).
11. Sengupta, S. et al. Enzyme molecules as nanomotors. *J. Am. Chem. Soc.* **135**, 1406–1414 (2012).
12. Dey, K. K. et al. Micromotors powered by enzyme catalysis. *Nano Lett.* **15**, 8311–8315 (2015).
13. Sengupta, S. et al. DNA polymerase as a molecular motor and pump. *ACS Nano* **8**, 2410–2418 (2014).
14. Zhao, X. et al. Substrate-driven chemotactic assembly in an enzyme cascade. *Nat. Chem.* **10**, 311–317 (2018).
15. Mohajerani, F., Zhao, X., Somasundar, A., Velegol, D. & Sen, A. A theory of enzyme chemotaxis: from experiments to modeling. *Biochemistry* **57**, 6256–6263 (2018).
16. Jee, A.-Y., Dutta, S., Cho, Y.-K., Tlusty, T. & Granick, S. Enzyme leaps fuel antichemotaxis. *Proc. Natl Acad. Sci. USA* **115**, 14–18 (2017).
17. Agudo-Canalejo, J., Illien, P. & Golestanian, R. Phoresis and enhanced diffusion compete in enzyme chemotaxis. *Nano Lett.* **18**, 2711–2717 (2018).
18. Zhang, Y. & Cremer, P. S. Interactions between macromolecules and ions: the Hofmeister series. *Curr. Opin. Chem. Biol.* **10**, 658–663 (2006).
19. Baldwin, R. L. How Hofmeister ion interactions affect protein stability. *Biophys. J.* **71**, 2056–2063 (1996).
20. Collins, K. D. & Washabaugh, M. W. The Hofmeister effect and the behavior of water at interfaces. *Q. Rev. Biophys.* **18**, 323–422 (1985).
21. Okur, H. I. et al. Beyond the Hofmeister series: ion-specific effects on proteins and their biological functions. *J. Phys. Chem. B* **121**, 1997–2014 (2017).
22. Monteiro, N., Martins, A., Reis, R. L. & Neves, N. M. Liposomes in tissue engineering and regenerative medicine. *J. R. Soc. Interface* **11**, 20140459 (2014).
23. Joseph, A. et al. Chemotactic synthetic vesicles: design and applications in blood–brain barrier crossing. *Sci. Adv.* **3**, e1700362 (2017).
24. Wilson, D. A., Nolte, R. J. M. & Van Hest, J. C. M. Autonomous movement of platinum-loaded stomatocytes. *Nat. Chem.* **4**, 268–274 (2012).
25. Peng, F., Tu, Y., Van Hest, J. C. M. & Wilson, D. A. Self-guided supramolecular cargo-loaded nanomotors with chemotactic behavior towards cells. *Angew. Chem. Int. Ed.* **54**, 11662–11665 (2015).
26. Jang, W.-S., Kim, H. J., Gao, C., Lee, D. & Hammer, D. A. Enzymatically powered surface-associated self-motile protocells. *Small* **14**, 1801715 (2018).
27. Guha, R. et al. Chemotaxis of molecular dyes in polymer gradients in solution. *J. Am. Chem. Soc.* **139**, 15588–15591 (2017).
28. Dey, K. K. et al. Chemotactic separation of enzymes. *ACS Nano* **8**, 11941–11949 (2014).
29. Xia, L. et al. Kinetic studies on Na^+/K^+-ATPase and inhibition of Na^+/K^+-ATPase by ATP. *J. Enzym. Inhib. Med. Chem.* **19**, 333–338 (2004).
30. Noske, R., Cornelius, F. & Clarke, R. J. Investigation of the enzymatic activity of the Na^+,K^+-ATPase via isothermal titration microcalorimetry. *Biochim. Biophys. Acta* **1797**, 1540–1545 (2010).
31. Kodama, A. et al. Migration of phospholipid vesicles can be selectively driven by concentration gradients of metal chloride solutions. *Langmuir* **33**, 10698–10706 (2017).
32. Shin, S. et al. Size-dependent control of colloid transport via solute gradients in dead-end channels. *Proc. Natl Acad. Sci. USA* **113**, 257–261 (2016).
33. Gupta, S., Sreeja, K. K. & Thakur, S. Autonomous movement of a chemically powered vesicle. *Phys. Rev. E* **92**, 1–8 (2015).
34. Anderson, J. L. Transport mechanisms of biological colloids. *Ann. NY Acad. Sci.* **469**, 166–177 (1986).
35. Velegol, D., Garg, A., Guha, R., Kar, A. & Kumar, M. Origins of concentration gradients for diffusiophoresis. *Soft Matter* **12**, 4686–4703 (2016).
36. Valdez, L., Shum, H., Ortiz-Rivera, I., Balazs, A. C. & Sen, A. Solutal and thermal buoyancy effects in self-powered phosphatase micropumps. *Soft Matter* **13**, 2800–2807 (2017).
37. Sengupta, S. et al. Self-powered enzyme micropumps. *Nat. Chem.* **6**, 415–422 (2014).
38. Anderson, J. L. Movement of a semipermeable vesicle through an osmotic gradient. *Phys. Fluids* **26**, 2871 (1983).
39. Nardi, J., Bruinsma, R. & Sackmann, E. Vesicles as osmotic motors. *Phys. Rev. Lett.* **82**, 5168–5171 (1999).
40. Leontidis, E. Investigations of the Hofmeister series and other specific ion effects using lipid model systems. *Adv. Colloid Inteface Sci.* **243**, 8–22 (2017).
41. Clarke, R. J. & Lu, C. Influence of anions and cations on the dipole potential of phosphatidylcholine vesicles: a basis for the Hofmeister effect. *Biophys. J.* **76**, 2614–2624 (1999).
42. Mclaughin, S., Bruder, A., Chen, S. & Moser, C. Chaotropic anions and the surface potential of bilayer membranes. *Bioehimica Biophys. Acta* **394**, 304–313 (1975).
43. Hatefi, Y. & Hanstein, W. G. Solubilization of particulate proteins and nonelectrolytes by chaotropic agents. *Proc. Natl Acad. Sci. USA* **62**, 1129–1136 (1969).
44. Hyde, A. M. et al. General principles and strategies for salting-out informed by the Hofmeister series. *Org. Process Res. Dev.* **21**, 1355–1370 (2017).
45. Zhang, Y., Furyk, S., Bergbreiter, D. E. & Cremer, P. S. Specific ion effects on the water solubility of macromolecules: PNIPAM and the Hofmeister series. *J. Am. Chem. Soc.* **127**, 14505–14510 (2005).
46. Zhang, Y. et al. Effects of Hofmeister anions on the LCST of PNIPAM as a function of molecular weight. *J. Phys. Chem. C* **111**, 8916–8924 (2007).
47. Melander, W. & Horváth, C. Salt effects on hydrophobic interactions in precipitation and chromatography of proteins: an interpretation of the lyotropic series. *Arch. Biochem. Biophys.* **183**, 200–215 (1977).

Methods

Thin-film hydration technique for liposome synthesis. We prepared monodisperse liposomes through the thin-film hydration and extrusion technique (Fig. 1c)[48]. We used L-α-phosphatidylethanolamine-*N*-(lissamine rhodamine B sulfonyl) (ammonium salt) (Egg Liss Rhod PE) to give the liposomes fluorescent characteristics.

1,2-distearoyl-sn-glycero-3-phosphoethanolamine-*N*-[biotinyl(polyethylene-glycol)-2000] (ammonium salt) (DSPE-PEG (2000) biotin) was used to get biotin functionality on the liposomes in order to attach enzymes on the external surface through biotin–streptavidin conjugation. The remainder of the lipid composition was made up of L-α- phosphatidylcholine (EPC) lipids.

Stock solutions of the lipids were prepared individually in chloroform. The lipids were pipetted in a molar ratio of 1:4:95 and added to a round bottom flask. The total concentration of lipids was maintained at a concentration of 1 mM. The solution was then dried using a rotavap to form a thin film of lipids and kept under vacuum for 2 h to ensure the removal of traces of chloroform solvent. The thin film was then rehydrated to 1 ml using 100 mM phosphate buffer (pH 7.2) and left stirring overnight for the self-assembly of phospholipids into liposomes. The suspension of polydisperse multilamellar vesicles was extruded using an Avanti Mini Extruder by passing them through a 0.1 μm polycarbonate membrane to obtain monodisperse unilamellar vesicles with diameters of 110 nm (polydispersity index (PDI) = 0.05) with free biotin ends.

The size and uniformity of the extruded liposomes were confirmed using a Malvern Zetasizer NS dynamic light scattering instrument (see Supplementary Fig. 1). Catalase and urease were attached to the outer membrane of the liposomes through biotin–streptavidin linkages. ATPase, being a transmembrane enzyme, was incorporated directly into the lipid bilayer during liposome formation.

Catalase and urease conjugation onto the surface of the liposome. The enzymes were conjugated onto the surface of the liposomes using the biotin–streptavidin linkage procedure (Fig. 1d)[49]. Enzyme biotinylation was performed using EZ-Link Maleimide-PEG2-Biotin for urease and EZ-Link Sulfo-NHS-Biotin for catalase in a 1:2 enzyme–biotin ratio. The starting enzyme concentration that was used was 5 μM. The biotinylated enzyme was then centrifuged at 4,500 r.p.m. for 5 min and washed three times with phosphate buffer using an Amicon Ultra centrifugal filter with a molecular weight cut-off (MWCO) of 10 kDa. The washed biotinylated enzymes were then conjugated with streptavidin in a 1:2 ratio and washed using the above procedure using an Amicon Ultra centrifugal filter (with a MWCO of 100 kDa). Subsequently, the biotin–streptavidin conjugated enzymes were mixed with the monodisperse liposomes for 1 h so that they attached onto the biotin-free ends of the liposomes. The liposomes were then washed using an ultra centrifugal filter (with a MWCO of 1000 kDa) to remove unattached enzymes. The size and uniformity of the extruded liposomes were determined using dynamic light scattering. The enzyme-coated liposomes were larger in size than the pure liposomes, which indicated that the enzymes were attached to the surface (see Supplementary Fig. 1).

Preparation of ATPase-bound liposomes. The ATPase liposomes were also prepared via the thin-film hydration technique following a previously reported protocol[50–52]. A 10 mg ml^{-1} lipid solution was prepared by adding EPC lipids to a chloroform solution. For labelling the vesicles, a 1 μM solution of Nile red dye was prepared in chloroform and added to the lipid solution and mixed thoroughly. Then 100 μl of this mixture was pipetted out in a round bottom flask and dried using a rotavap at 37 °C for 1 h until a thin film was formed. Subsequently, the flask was placed under vacuum overnight to remove trace solvent impurities. The completely dried lipid film was hydrated with ~1 ml of buffer under N_2 atmosphere and stirring for 1 h. It was then rehydrated by adding 5 ml of 1 μM ATPase solution with initial stirring in a N_2 atmosphere and incubating overnight at ~10 °C. In this step, the ATPase enzyme was reconstituted in the lipid bilayer via hydrophobic interactions with its transmembrane α helices. In the final step, the excess dye as well as unattached enzyme molecules were removed by dialysis membrane filtration and subsequently the residual solution was subjected to extrusion to yield 100-nm-sized unilamellar liposomes.

Liposome chemotaxis in the imposed gradients. A three-inlet one-outlet PDMS channel with dimensions of 4 cm (length) × 360 μm (width) × 100 μm (height), was used to visualize liposome chemotaxis under confocal microscopy (Fig. 1b)[9,27]. The shifting mode of chemotaxis was primarily used, where the enzyme-coated liposomes were flown through the middle channel, and the substrate and buffer were flown in each of the side channels, respectively. With known flow rates and channel dimensions, the diffusion time and interaction time between the liposomes and substrates can be controlled. Optical scans were taken across the channel width at a distance of 38 mm from the inlet (~34 s residence time) using a confocal laser scanning microscope. Chemotactic shifts of liposomes were measured perpendicular to the direction of flow.

Data availability

The data that support the findings of this study are available from A.Sen upon reasonable request.

References

48. Frisken, B. J., Asman, C. & Patty, P. J. Studies of vesicle extrusion. *Langmuir* **16**, 928–933 (2000).
49. Loughrey, H., Choi, L., Wong, K. & Cullis, P. R. Preparation of streptavidin-liposomes for use in ligand-specific targeting applications. *Liposome Technol.* **III**, 163–178 (1993).
50. Walde, P. & Ichikawa, S. Enzymes inside lipid vesicles: preparation, reactivity and applications. *Biomol. Eng.* **18**, 143–177 (2001).
51. Akashi, K. I., Miyata, H., Itoh, H. & Kinosita, K. Preparation of giant liposomes in physiological conditions and their characterization under an optical microscope. *Biophys. J.* **71**, 3242–3250 (1996).
52. Ghosh, S. et al. Motility of enzyme-powered vesicles. *Nano Lett.* **19**, 6019–6026 (2019).

Acknowledgements

The work was supported by the Center for Chemical Innovation funded by the National Science Foundation (grant no. CHE-1740630). P.S.C. and D.V. acknowledge the National Science foundation for funding their work (grant nos. CHE-1709735 and CBET-1603716, respectively)

Author contributions

The work was conceived by P.S.C., D.V. and A.Sen. A.Somasundar, S.G., F.M., L.N.M. and T.Y. performed the experiments. F.M. carried out the modelling. All the authors contributed to the discussion of results and the writing of the manuscript.

Competing interests

The authors declare no competing interests.

Additional information

Supplementary information is available for this paper at https://doi.org/10.1038/s41565-019-0578-8.

Correspondence and requests for materials should be addressed to P.S.C., D.V. or A.S.

Peer review information *Nature Nanotechnology* thanks Jinyao Tang and the other, anonymous, reviewer(s) for their contribution to the peer review of this work.

Reprints and permissions information is available at www.nature.com/reprints.